A Computational Study to Determine and Compare the Structural and Elastic Properties of MgO, CaO and the Earth Material at PREM Pressures up to the Outer Core's Limits of the Earth

Benatallah Nassiba[1], Tlili Salah[2], Kaddour Abdelmadjid[3], Medjahed Driss Meddah[4], Achouri Abderrahim[5], Mohammed Said Nedjimi[6],Medjadji Nassira[7], Mebrouki Noura[8]

[1,2]Univ. Ouargla, Fac. Mathematics and Material Sciences, Lab. Development Of New And Renewable Energies In Arid And Saharan Zones Laboratory (LARENZA), 30000, Ouargla (Algeria).

[3]Unité de Recherche Appliquée en Energies Renouvelables, URAER, Centre de Développement des Energies Renouvelables, CDER, 47133, Ghardaïa(Algeria).

[4]Mechanical Engineering Department, University Center Salhi Ahmed Naama, Naama45000(Algeria).

[5]Laboratoire de Développement des Energies Renouvelables dans les Zones Arides et Sahariennes, Département de Physique, Université d'Ouargla, 30000 Ouargla(Algeria).

[6]Univ. Ouargla, Fac. Mathematics and Material Sciences, Lab. Valorisation and Promotion of Saharan Resources Laboratory (VPRS), 30000, Ouargla(Algeria).

[7]Electrical Engineering Department, University Center Salhi Ahmed Naama, Naama45000(Algeria).

[8]Univ Ouargla, Fac. Mathematics and Material Sciences, Lab. Radiation and Plasmas and Surface Physics Laboratory (LRPPS), Ouargla(Algeria).

Received: 02 July 2023 Revised: 10 September 2023 Accepted: 10 October2023 Published: 05 November, 2023

Email Corresponding Author: tlilisalah2007@gmail.com

Abstract:

By changing the pressure up to 140 GPa, we aimed in this work to study some parameters of the structural and elastic properties of MgO and CaO and compare them with those provided by the PREM model. This was calculated using the DFT method, the GGA approximation, as we chose from among several functions the modern function PBEsol. Starting with geometric optimization, we confirmed that the phase transformation of calcium oxide from phase B1 to B2 occurs at 59.2 GPa, while manganese oxide remains stable in its first phase, B1. Despite the slight difference in

our results from the previous study, whether experimental or computational, especially at zero pressure, the agreement confirms the validity of these results. Also, after we chose the degree of the polynomials most appropriate to the change of these parameters with changes in pressure, we were able to accurately compare the parameters of these two oxides and between them and what is provided by the PREM model, in addition to determining the values of these parameters at the basic discontinuities in the subsurface to contribute to the global data base.
Keywords: structural properties, elastic properties, MgO, CaO, PREM model

Tob Regul Sci. ™ 2023 ;9(2) : 712-746
DOI : doi.org/10.18001/TRS.9.2.45

Introduction

Seismology is a science specialized in studying the propagation of waves in the layers that make up the planets, whether they are liquid or solid. The waves here are called seismic waves [01]. It also studies rocks in terms of the forces affecting them and exposes them to stresses whose strength may lead to fractures in these rocks, resulting in energy spreading in the form of waves [02].

This science includes several branches, including seismology the globe, which studies the depths of the planets in terms of their formation and composition through data resulting from earthquakes. His scientists have proposed two methods to study the inner layers [03], inverse and direct method.

The first, also called modern seismology [04], is based on the study of materials under the thermodynamic conditions of the Earth's layers [05]. Assuming that it is a group of rocks or minerals composed of crystals, pressure at depth is often used as a variable while neglecting the effect of temperature in the face of high pressure changes [05]. Experimentally, some use diamond cells as a tool for producing high pressure and lasers as a heating tool [06], but such experimental techniques are difficult to achieve. Therefore, it was necessary to simulate these methods by developing theoretical methods using a computer for calculation, and thus many programs were available as virtual laboratories. These programs can identify many of the properties of the studied materials, through which other properties can be deduced to know the presence and nature of the materials in the inner layers.

As for the second, it relies on the spectra consisting of signals of different waves resulting from natural earthquakes or powerful explosions and recorded by a seismograph [07]. Analyzing these spectra in various special ways made it possible to suggest a good division of the Earth's layers by determining their depths and physical components. Therefore, many models were proposed, including the PREM (Preliminary Reference Earth Model (1981)) [08]. This one-dimensional model with spherical symmetry was preceded by the Jeffress-Bollen model (1939) and is also used, but to a lesser extent. Today, several different models are available that are still less used, the most important of which are LASP91 (1991) and Ak135 (1995) [09].

Through the PREM model, it was possible to provide a picture of the pressure change (Figure 1), the density of the material, and the longitudinal and transverse wave velocities depending on the depth (Figure 2). Moreover, it was found that the Earth consists of multiple, overlapping, concentric layers. From its surface, where we live, to its center, it is divided as follows: The crust, which includes the land and ocean, the mantle, which includes the upper and lower parts, and finally the core, which is external and internal, These layers are interspersed with interruptions that are as follows: The Mohorovichi (Moho) discontinuity separates the crust from the mantle, the Gutenberg discontinuity, or D'' layer, separates the mantle from the core, and the Lehmann discontinuity separates the two parts of the core. The most important measurements for these divisions can be found, which are: Depth, pressure, material density, and longitudinal and transverse wave velocities are in Table 1 below [08].

These divisions consist of multiple minerals such as peridotites, olivine, pyroxène, spinelle, and magnesiowüstite. These minerals are formed by the fusion of oxides, or so-called pure electrodes, such as MgO, FeO, BaO, CaO, Al2O3, etc. [10], and these oxides can also exist individually [04]. In this work, we are interested in manganese oxide, MgO, or what is known as periclase, and calcium oxide, CaO. Many studies, whether experimental or theoretical, have been interested in studying them, as: they were studied alone and in series in [52–11] and [62–53], and they were studied together only in [63–66], and moreover, they were studied with other oxides in [69–74]. In addition to studying the first oxide with Wüstite or FeO in a study [67], the second oxide was studied in the work of [68]. These two oxides are of great importance in the formation of many minerals in the Earth's inner layers [10], especially MgO, which is included in the formation of Magnésiowüstite minerals, the main component of the Earth's lower mantle [78–75], and is also included in the formation of MgSiO3 minerals [80–79].

These studies reported that these two oxides, under normal thermodynamic conditions, stabilize in the cubic structure of the NaCl type, or what is known as the B1 phase with the space group Fm-3m (225), like the rest of the mono-oxides or the pôle pure. Where the positive ions are located in principle, that is, at (0,0,0), while the oxygen ions occupy the positions (0.5,0.5,0.5) (see Figures 3 and 4). When these thermodynamic conditions change to a certain extent, the crystal changes its phase and inevitably settles into another phase, and this is what actually happens to these two oxides, especially when the pressure increases only, for example. Most of these studies indicate that these two oxides transform into the same phase with the constant occupation of the ions in the same positions in the previous structure, which is the B2 phase with a cubic structure of the type CsCl with the space group Pm-3m (221). However, there is a clear and significant difference in the area of stability of each of them in its first phase, as these studies have shown that calcium oxide has a lower area of stability than the other oxide, meaning that its transformation pressure is lower. Most of these studies dealt with structural properties and elasticity, but this was in varying forms, as some dealt with some properties rather than others under conditions of varying pressure and temperature as well.

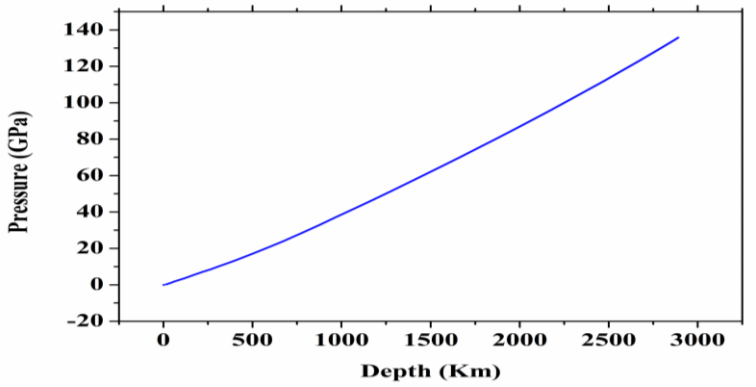

Fig 1. Pressure changes in the subsurface with depth changes determined in the work of [08] up to the Gothenbur

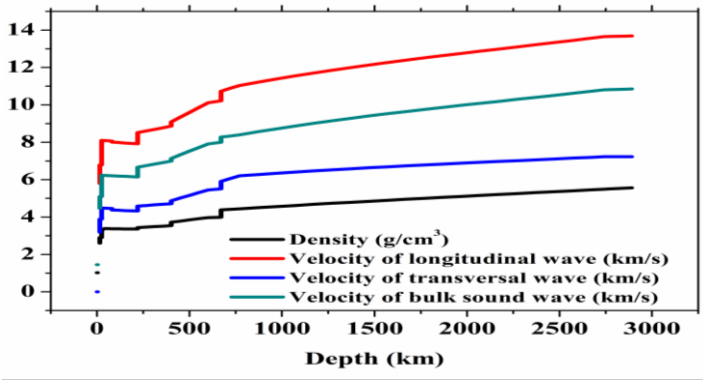

Fig 2. Changes in density, velocities of longitudinal and transverse waves, and sound pressure with depth up to the Gothenburg area

Table 1. Density values, longitudinal and transverse wave velocitys, and acoustic pressure from the PREM model determined in the work of [08] at the boundaries of the Earth's interior layers up to the Gothenburg region

	Depth(km)	Pressure (GPa)	Density(g/cm3)	Velocity of longitudinal wave(km/s)	Velocity of transversal wave(km/s)	Velocity of bulk sound wave (km/s)
crust	0	0	1,02	1,45	0	1,45
	80,0	2,4539	3,38	8,07	4,46	6,21
Upper mantle	80,0	2,4546	3,38	8	4,38	6,2
	670,0	23,8334	3,99	10,22	5,5	8
Lower mantle	670,0	23,8342	4,38	10,73	5,91	8,28
	2891	135,7509	5,57	13,69	7,23	10,85

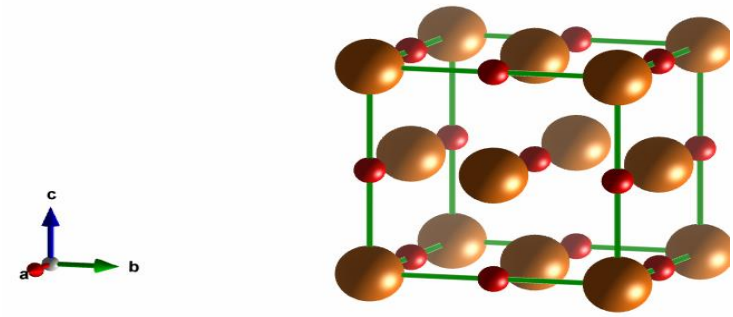

Fig 3. Crystal structures of phase B1 in which MgO and CaO can settle, prepared using the VESTA program The large, golden-colored balls represent Mg^{+2} or Ca^{+2} ions, while the small, red-colored balls represent O^{-2} ions.

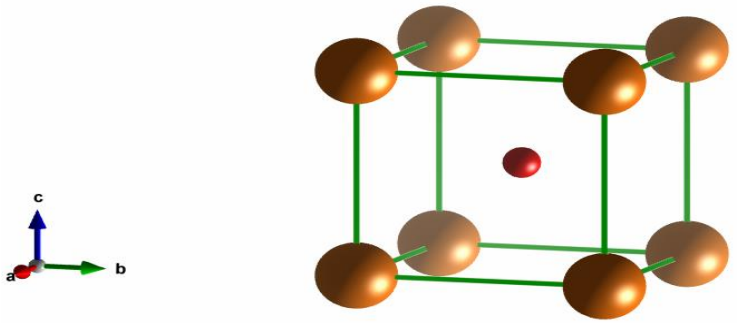

Fig 4. Crystal structures of phase B2 in which MgO and CaO can settle, prepared using the VESTA program The large, golden-colored balls represent Mg^{+2} or Ca^{+2} ions, while the small, red-colored balls represent O^{-2} ions.

In these papers, we will mathematically re-examine all these properties of these two oxides up to the borders of the Gutenberg transition zone, that is, until the pressure is 135,7509 GPa. Focusing on the following parameters, starting with the geometric optimization, the change of the primitive cell parameter, the primitive cell volume, the volume ratio, and the density of the material are included in the structural properties. And the elastic constants, the bulk and shear modulus, the velocities of longitudinal, transverse and the bulk sound waves are parameters related to elastic properties. But at accurate pressure values, which are values in the PREM seismic model, compare their values with those available in this model, if any. With a focus on determining the values of these parameters at the boundary intervals of the Earth's layers, starting from the crust, where the pressure is estimated at 0 GPa. Our calculations are also compared to the results of other studies, especially those that are consistent with them. This will be after discussing the study method and finally arriving at a conclusion presenting our most important results.

2. Methodology:

The most commonly used methods are the so-called "ab-initio" methods based on partial dynamics [82], methods based on statistical physics (vibrational methods) [05], and methods based on thermodynamics [83].

For our part, we applied the density functional theory (DFT), which is one of the most important methods used in theoretical physics and chemistry, and through it we can determine the properties of a multi-particle system, the total energy of the system, the electronic density of the orbitals, and the physical and optical parameters of the matter, etc.,, and it is one of the most widely used methods in quantum calculations for solving the Schrödinger equation due to the possibility of applying it to various systems (multivariable) [84]. The program CASTEP is based on this theorem [85], which uses several approximations. We used the generalized gradient approximation (GGA) [87–86], which has evolved and become more powerful due to its multiple uses. In 2008, the PBEsol approximation used here and explained in more detail in [88] appeared. We adopted the limits of the Brillion region of 10 x 10 x 10 and estimated the cut-off energy at 630 eV. These values enable us to provide a very close calculation with very reliable results.

We have used Brillouin zone sampling at 10 x 10 x 10 and an energy cut-off equal to 630 eV. These values ensure good calculation convergence with respect to reliable results. More than that, mathematically, the change of any function within a certain range can be approximated by another function. Among these functions are polynomials that are widely used. The pattern often defined as generation or polarization [89] can be used here, where it can be written:

$$f(x) = P_n(x) = \sum_{i=0}^{n} a_i x^i \qquad (1)$$

To calculate the values of the coefficients for the polynomials of degree n that must be determined, one of the following numerical methods can be adopted: Lagrange's method, finite difference method, Newton's method, partitioned difference method, diving method, Stirlich's method, Bessel's method, and inverse polarization method in the cases of regular and irregular points This method is what we use to determine the change in the studied parameters with changes in pressure.

3. Results and interpretation:

3.1. Geometric Optimization:

The calculation we did is at absolute zero, so the change in free energy ΔG of crystal formation is equal to the enthalpy H, or enthalpy of formation, where:

$$\Delta G = H + TS = H + (0)S = H \qquad (2)$$

where T is the temperature and S is the entropy of formation. This confirms the validity of our calculation of enthalpy, which is calculated in the B1 and B2 phase structures for both MgO and CaO in the field of this study between 0 and 140 GPa. The enthalpy of formation resulting from this calculation decreased in all phases for both oxides in an almost linear manner, but decreased at different velocities. So this enthalpy is limited to 13.15 eV and 12.45 eV for the first oxide phase, respectively, while it is limited to 16.31 eV and 14.56 eV for the second oxide phase, respectively (see the values of the first line of Table 3).

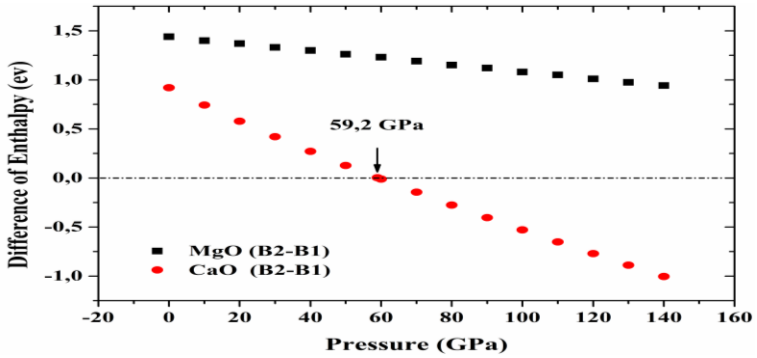

Fig 5. Changes in the enthalpy difference of the MgO and CaO structures in their B1 and B2 phases with changes in pressure.

Moreover, by dealing with the difference in the values of this enthalpy between the two phases of each oxide, its value in the first phase is the reference, that is, the zero values. This difference, whose change with pressure changes is shown in Figure 5, also decreases approximately linearly with the increase in pressure. For manganese oxide, according to the same form, the decrease is slow compared to other oxides, which makes the value of the difference always positive. This is consistent with all previous studies, especially the work of [15], who experimentally determined that the phase transition occurs at a pressure of approximately 205 GPa, or the theoretical work of [16], who found that the phase transition occurs at approximately 202 GPa. This result confirms the stability of MgO in its first phase throughout the entire study area, meaning that this oxide, up to the boundaries of the Earth's outer core, remains stable in this structure.

As for CaO, the decrease is faster, as always shown in Figure 5. This decreasing velocity leads to a change in the difference sign for this oxide between the pressures of 50 and 60 GPa, which means that there is a phase transformation in this range. Through a simple mathematical calculation, we found that the shift more accurately falls between 59 and 60 GPa, so we were forced to recalculate for the 59 GPa value of pressure. At this pressure, we found that this difference is positive with a very small value of 2.86 meV, meaning that the structure of the table salt of calcium oxide is still stable at this pressure. After entering the results at this pressure into the simple mathematical calculation, it appears that the phase transition more accurately occurs at a pressure of 59.2 GPa. This result is very close to the degree of agreement with what was found experimentally in the work of [55], as it is 0.8 GPa less than what was determined in this study. Based on the relationship of pressure to Earth's depth, it can be said that the phase transformation of this oxide takes place at a depth of 1435 km from the Earth's crust, that is, in the Earth's lower mantle at a distance of 1456 km from the Gutenberg region, which represents the boundary separator between this part of the mantle and the outer core.

3.2. Study of structural characteristics:

3.2.1. Structural changes and equation of state:

Figures 6–8 represent the changes in the crystal lattice constant, its size, and the percentage of this size with changes in pressure, respectively. When the crystal is compressed hydrostatically, each of

these curves decreases, as it is also noticeable for all of these parameters that in the field of stability of the first phase of calcium oxide, this decrease is faster for both oxides. This can be confirmed by the values shown in Table 3 and also by examining the values of the differences in the values of these parameters. Considering the same arrangement, whether in the parameters or for the two oxides, these differences are: In the range between 0 and 60 GPa (MgO) or 59 GPa (CaO), it is 0.23 A, 4.02 A3, 0.21 and 0.30 A, 6.58 A3, 0.24, and in the range between 60 and 140 GPa, it is 0.14 A, 2.23 A3, 0.12 and 0.15 A, 2.86 A3, 0.11.

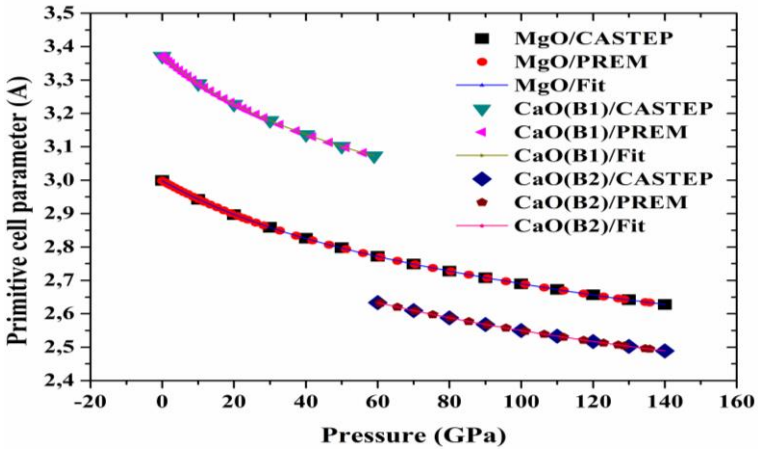

Fig 6. Changes in network constant values; Calculated using the CASTEP program, calculated at PREM pressures and filtering polynomials suitable for the MgO and CaO structures in their B1 and B2 phases with changing pressure.

At 0 GPa, for example, the value of the lattice constant of the conventional manganese oxide cell calculated here is higher than that obtained in the study [16] with the value 0.008 A, meaning that there is a great agreement between the two values. But for the second oxide, for example, at the same pressure, the value of this constant calculated here is less than that which was obtained in the research paper by [11] with a value of 0.06 A. There is also a great agreement, but it is less than what resulted for the first oxide. At this pressure, the value of this constant for calcium oxide is about 0.4 A higher than that for other oxides. With increasing pressure until the phase transition pressure, the difference decreases very slowly. But after the transformation pressure, the value of manganese oxide is lower by about 0.14 A. This difference is approximately constant at all pressures in this phase. The lattice constant changes in a polynomial manner of the fourth degree (see Table 3) with pressure, whether for the calcium oxide or manganese oxide phases. This approximation enables us to determine its values at all depths of the Earth's interior, that is, at PREM pressures, especially at the most important separations between the layers. The internal floor is as presented in Table 3.

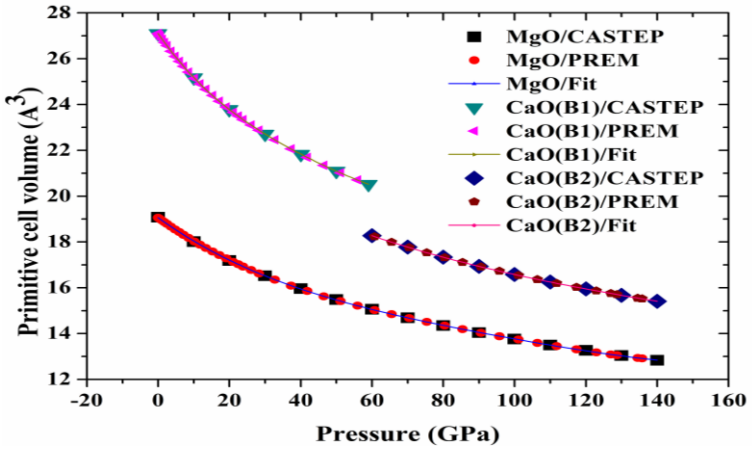

Fig 7. Changes in initial cell size values calculated using the CASTEP program, calculated at PREM pressures, and filtering polynomials suitable for the MgO and CaO structures in their B1 and B2 phases with changing pressure.

In the same table 3, it is also possible to present the values of the initial cell volume of the oxide structures at the most important intervals between the internal layers of the Earth, since after determining the values of the polynomial coefficients expressing the change of this volume with the change in pressure, the values of this volume can be easily calculated at the pressure values of the PREM model. These polynomials have coefficient values listed in Table 2, where their degrees are: The sixth is for MgO, and the fourth is for each of the two CaO phases. The values of this size for calcium oxide are always the highest, but the difference between the values of the two oxides is similar to that resulting from the lattice constant, where: at zero pressure, this difference is estimated at 8.02 A3, and at 140 GPa, it is estimated at 2.58 A3. Moreover, at this pressure, the value of this volume is less than that determined in the work of [59] by 0.56 A3, that is, with a relative error of approximately 3.63%, meaning that there is a fairly good agreement.

As for the volume ratio, which takes the value of one at 0 GPa, it results from dividing all the volumes calculated at different pressures by the value of the volume at this pressure, V0. After this pressure, this percentage for manganese oxide is always higher than that for oxide II, especially in its second phase, where the difference is much greater despite its decrease with increasing pressure. To confirm this, this difference takes the following values: 0.03, 0.12, and 0.10, respectively, at the following pressures: 50, 60, and 140 GPa. The values of this ratio can be identified at all depths of the earth, which are represented by the pressure values in the PREM model, including what is listed in Table 3 regarding the values of this ratio at the most important intervals between the internal layers of the earth. This is, of course, after determining the coefficients of the polynomials (see Table 2) expressing the change of this parameter with changes in pressure, whose degrees are second degree for all phases of calcium oxide and fourth degree for manganese oxide.

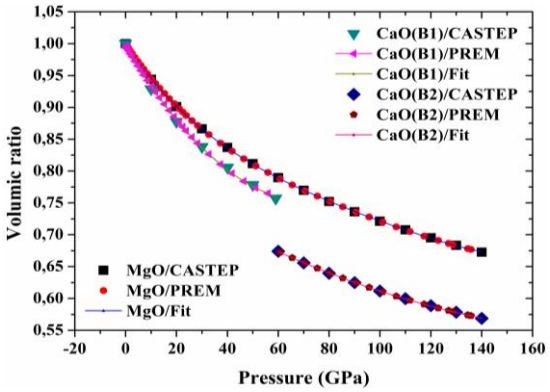

Fig 8. Changes in volume ratio values calculated using the CASTEP program, calculated at PREM pressures, and filtering polynomials suitable for the MgO and CaO structures in their B1 and B2 phases with changing pressure

Table 2.Values of polynomial parameters suitable for changes in the lattice constant, primary cell size, density, elastic constants and parameters, longitudinal and transverse wave velocities, and acoustic compression of MgO and CaO with changing pressure

		Degree of polynomial	Polynomial coefficients								
			a8	a7	a6	a5	a4	a3	a2	a1	a0
Lattice parameters (A)	MgO	4	/	/	/	/	8,04E-10	-3,21E-07	5,29E-05	-59,71E-04	3,00
	CaO/B1	4	/	/	/	/	9,06E-09	-1,71E-06	14,32E-05	-94,34E-04	3,37
	CaO/B2	4	/	/	/	/	2,05E-10	-1,20E-07	3,051E-05	-50,67E-05	2,85
Current cell volume (A^3)	MgO	6	/	/	1,54E-12	-8,09E-10	1,76E-07	-2,13E-05	17,02E-04	-12,11E-02	19,08
	CaO/B1	4	/	/	/	/	2,57E-07	-4,77E-05	38,58E-04	-22,60E-02	27,10
	CaO/B2	4	/	/	/	/	5,55E-09	-3,18E-06	77,40E-05	-11,59E-02	23,05
V/V_0	MgO	4	/	/	/	/	9,20E-10	-3,62E-07	5,80E-05	-58,74E-04	1,00

	CaO /B1	2	/	/	/	/	/	/	4,51E -05	-66,55 E-04	1,00
	CaO /B2	2	/	/	/	/	/	/	6,04E -06	-25,11 E-04	0,80
Density (g/cm^3)	Mg O	4	/	/	/	/	-1,99E -09	8,09E -07	-14,15 E-05	21,58 E-03	3,51
	CaO /B1	4	/	/	/	/	-1,82E -08	3,56E -06	-32,42 E-05	29,15 E-03	3,44
	CaO /B2	4	/	/	/	/	-5,87E -10	3,75E -07	-10,57 E-05	23,84 E-03	3,97
C_{11} (GPa)	Mg O	2	/	/	/	/	/	/	-6,84E -03	8,69	287 ,41
	CaO /B1	2	/	/	/	/	/	/	-1,17E -02	9,45	226 ,93
	CaO /B2	2	/	/	/	/	/	/	-5,08E -03	4,96	411 ,31
C_{12} (GPa)	Mg O	8	2,02 E-13	-1,21E-10	2,98E-08	-3,89E -06	2,88E -04	-1,20E -02	0,25	-0,53	88, 03
	CaO /B1	2	/	/	/	/	/	/	-6,05E -04	1,44	58, 44
	CaO /B2	2	/	/	/	/	/	/	-6,97E -04	3,18	-15, 9
C_{44} (GPa)	Mg O	6	/	/	-2,09E-12	2,24E -09	-6,89E -07	1,03E -04	-1,04E -02	0,98	138 ,54
	CaO /B1	4	/	/	/	/	-3,90E -07	1,01E -04	-1,09E -02	0,12	77, 26
	CaO	2	/	/	/	/	/	/	-	2,04	-

	/B2								3,96E-03		16,86
Bulk modulus (GPa)	MgO	6	/	/	2,25E-10	-9,94E-08	1,66E-05	-1,28E-03	3,98E-02	3,48	153,17
	CaO/B1	4	/	/	/	/	-4,95E-08	2,28E-05	-4,31E-03	4,11	114,6
	CaO/B2	2	/	/	/	/	/	/	-2,16E-03	3,78	126,5
Shear modulus (GPa)	MgO	4	/	/	/	/	-1,78E-07	7,63E-05	-1,41E-02	2,25	121,13
	CaO/B1	4	/	/	/	/	-1,06E-06	2,48E-04	-2,52E-02	1,6	79,87
	CaO/B2	4	/	/	/	/	-4,01E-07	1,68E-04	-2,82E-02	3,58	-0,74
Velocity of longitudinal wave (km/s)	MgO	4	/	/	/	/	-1,12E-08	4,52E-06	-7,30E-4	07,10E-2	11,32
	CaO/B1	4	/	/	/	/	-9,93E-08	1,91E-05	-1,52E-3	6,28E-2	9,35
	CaO/B2	4	/	/	/	/	-1,84E-08	8,17E-06	-1,46E-3	0,15	5,42
Velocity of transversal wave (km/s)	MgO	5	/	/	/	-8,60E-11	-5,91E-09	2,33E-06	-3,65E-04	3,39E-02	5,88
	CaO/B1	4	/	/	/	/	-4,53E-08	8,80E-06	-6,99E-04	2,71E-02	4,82
	CaO/B2	6	/	/	-2,12E-11	1,35E-08	-3,52E-06	4,84E-4	-3,68E-2	1,49	-19,98
Velocity of bulk sound wave	MgO	5	/	/	/	3,87E-13	-1,01E-08	5,06E-06	-7,00E-04	6,15E-02	9,05

(km/s)											
	CaO /B1	4	/	/	/	/	-8,51E-08	1,62E-05	-1,29E-03	5,50E-02	7,52
	CaO /B2	6	/	/	-3,01E-11	1,92E-08	-5,04E-06	6,93E-4	-5,29E-2	2,15	-28,09

The change in pressure as a function of this parameter presents the equation of state, the most important of which is that based on the definition of ductility by Barkh-Markhan [90], and the introduction is as follows:

$$P = \frac{3B_0}{2}\left[\left(\frac{V}{V_0}\right)^{-\frac{7}{3}} - \left(\frac{V}{V_0}\right)^{-\frac{5}{3}}\right]\left[1 + \frac{3}{4}(B_0' - 4)\left(\left(\frac{V}{V_0}\right)^{-\frac{2}{3}} - 1\right)\right] \qquad (3)$$

This equation enables us to determine the value of the bulk modulus B and its derivative B' = dB/dP at zero pressure. After calculation and using the values calculated by the program, we found that their values, respectively, are: 156.2 GPa and 4.08 for MgO, 115.5 GPa and 4.34 for CaO in its first phase, and finally 50 GPa and 5.75 for the same oxide in its second phase. However, their values, when using the values calculated at PREM pressures, increase for the volumetric compression factor while decreasing for its derivative. Taking the same sequence as before, the amounts of increase and decrease are as follows: 0.8 GPa and 0.4; 7.3 GPa and 0.59; 0.8 GPa and 0.09. Through this comparison, it appears that the polynomial chosen to calculate the values at PREM pressures in the case of manganese oxide is more reliable, while in the case of calcium oxide in its first phase, it is less reliable.

Comparing the results of our calculations using the program with previous studies, in the case of manganese oxide, the value of the compression modulus mentioned above is 2.02 GPa and 3.2 GPa, respectively, higher than the value implied by computational work [36] and experimental work [28], but it is lower in value. 3.8 GPa from the value found in the following two publications [79] and [42], experimental and computational, respectively. As for the value of its derivative, it matches that published by the computational works of [65] and [42], while this value is limited to that presented by the following two experimental studies: [32] and [76], between values 0.6 and 0.01. Just to note, the values calculated at PREM pressures remain within the same range as these studies because the values of this parameter and its derivative with respect to pressure are very close. In the case of calcium oxide in its second phase, our calculations cannot be compared with the rest of the work because we only calculated within the limits of the stability of this phase, that is, between 60 and 140 GPa.

Either for its first phase:

The compression modulus value calculated using the program or those calculated at the PREM pressures mentioned above are close to superior to those calculated in my work [69] and [65],

with values of 0.5 GPa and 0.8 GPa, respectively. On the other hand, these two values are close to those measured experimentally in the work of [54] and [56], as this value measured in the first work exceeds that calculated using the program by an amount of 0.5 GPa, and that value measured in the second work is less than that calculated at the PREM pressures. By 6.7 GPa.

As for the value of the derivative of this parameter in relation to pressure, it is very close to that calculated using the program, with a value of 0.01 superior to that specified in the theoretical study prepared by [71], while its value calculated at PREM pressures is also close to 0.15 superior to that value. The value was theoretically proven in a study [81]. Moreover, compared to experimental works, we find that the value of the derivative of this parameter with respect to pressure agrees with an estimate of 0.08 superior to the work of [55] for the value calculated by the program, and we also find it agrees and is less than that of [54] for the value calculated at PREM pressures by the amount of 0.35.

3.2.2. Density:

Density or volumetric mass is also one of the parameters provided directly by the program used in our calculations, and it is calculated for single oxides as follows:

In the case of the structure of NaCl, this is done using the following relationship:

$$\rho = 6.64\frac{M_O + M_X}{V_C} \qquad (4)$$

In the case of the structure of CsCl, this is done using the following relationship:

$$\rho = 1.66\frac{M_O + M_X}{V_C} \qquad (5)$$

where: VC is the volume of the conventional cell, taken in cubic centimeters, and MX and MO are the molar masses of the positive anion and the oxygen ion, respectively, taken in grams.

Through this relationship, it is logical that the change in density values is completely opposite to the size of the cell, whether it is basic or conventional, in addition to being affected by the difference in the mass of the positive molar that does not change with pressure, so it inevitably always increases as the pressure increases, that is, the more we penetrate into the interior of the earth. This is confirmed by what resulted from our calculations, as shown in Figure 9, which represents the density change of oxide with changing pressure. Through these calculations and in the areas of stability of the oxide phases, we find that the density values change in areas of width of 1.71, 1.10, and 0.95 g/cm3 for MgO and CaO in their first and second phases, respectively. It can also be easily proven that, over the entire study range of pressure, the range of change of this density for calcium oxide is approximately 0.9 g/cm3 greater than for its counterpart, which is for manganese oxide. The density value of manganese oxide is higher than that of calcium oxide, with a difference estimated at 0.07 g/cm3 at zero pressure, that is, within the surface of the earth's crust. This difference, starting from this pressure, begins to decrease until the pressure falls between the pressure values of 10 and 20 GPa, that is, at a depth in the Earth's upper mantle. After the last pressure, the situation reverses, and the value of the specific density of the first oxide

is always lower, with an ever-increasing difference, from the amount of 0.02 at the pressure of 20 GPa to the amount of 0.09 at the pressure of 50 GPa for the first phase, and from the amount of 0.65 at the pressure of 60 GPa until the amount of 0.83 at the pressure of 140 GPa for the other phase. All of this indicates that the increase in density of calcium oxide is faster than that of its counterpart of this second oxide, on the one hand, and on the other hand, the development of this parameter is faster in the first phase of this oxide than in its second phase.

Comparing the values of our calculations at zero pressure for the density of manganese oxide with those resulting from the work calculation [26], we found that they are very close, with the difference estimated at 0.02 g/cm3. The same is true for the second oxide, where the comparison is made with that value determined in the work of [70], where the difference is estimated at 0.24 g/cm3, meaning the compatibility is less in this case. However, it is unfortunate that experimental values, at least under the same conditions, are not available for comparison, and this is for oxides.

To determine the density values for each oxide at PREM pressures, the fourth degree of each polynomial was estimated for its change with pressure (see Table 2).

Through this determination, a range was found in which the two oxide density values could be applied with better accuracy than those previously determined using the values calculated by the program. We found that the depth at which this correspondence can occur is between the two pressures (355 km, 11.7702 GPa) and (400 km, 13.352 GPa), that is, approximately in the middle of the Earth's upper mantle. In addition, it has become possible to determine the values of this density at the most important internal Earth in tersection, which are specified in Table 3.

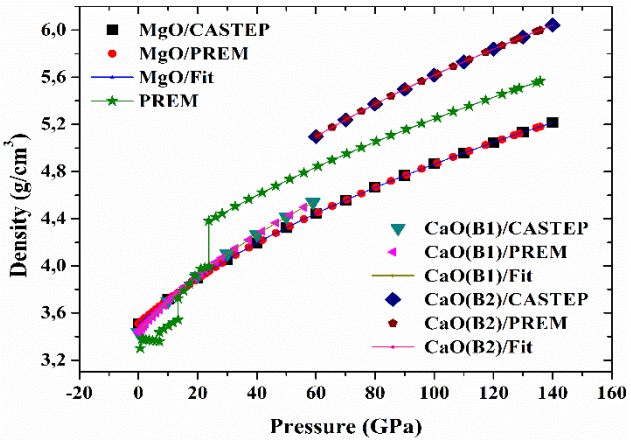

Fig 9. Changes in density values calculated using the CASTEP program, calculated at the PREM pressures, determined from the PREM model, and the appropriate filtering polynomials for the MgO and CaO structures in their B1 and B2 phases with changing pressure.

The density study is considered the first reading in seismic observations, so determining its values at PREM pressures is necessary so that the comparison between it and those available in the same model is accurate; that is, each value has a value. If the density in this model represents the density

of the earth's matter, in other words, this comparison is based on the material content of the earth's interior.

In an inaccurate general view, the density values of Earth matter are lower than those of oxides, starting from the surface of the earth's crust until equal values occur. This appears for manganese oxide between the two pressures (450 km, 15.2251 GPa) and (500 km, 17.1311 GPa), with a decreasing difference until the pressure (40 km, 1.1239 GPa) and oscillating after that. As for calcium oxide, this appears between the two pressures (500 km, 17.1311 GPa) and (550 km, 19.0703 GPa), with a decreasing difference also in two fields, the first of which is the same as the previous field mentioned in favor of the other oxide. The second of which is from the beginning of the Earth's lower mantle, that is, from the pressure (670 km, 23.8342 GPa). The density of this oxide over its entire second phase is higher than that of the Earth substance, with an increasing difference. Density values for the second oxide in the Earth's lower mantle are lower than those for the Earth's matter, with a difference that decreases until pressure (2671 km, 122.9719 GPa), where the difference begins to increase slightly until the boundaries of the Earth's outer core.

3.3.Study of elastic properties:

3.3.1. Elastic constants:

The elastic constants of materials provide a link between the mechanical and dynamic behavior of crystals and give important information regarding the nature of the forces acting on solid materials [91]. After knowing the sum of the structures present when changing pressure, we can know the elastic constants Cij, as each crystal structure has special constants, as is known in the physics of solid bodies. In a homogeneous elastic medium with infinite deformations, stresses and deformations are linearly related according to Hooke's law. In the general case, it is given in affective form.

$$\sigma_{ij} = C_{ijkl}.\varepsilon_{kl} \qquad (6)$$

An inverse relationship can be defined:

$$\varepsilon_{ij} = s_{ijkl}\sigma_{kl} \qquad (7)$$

where: σ_{ij} and $\varepsilon_{ij}$are the effects of stress and deformation, C_{ijkl} and $s_{ijkl.}$ the elastic constants are respectively 4th order effects of the elasticity coefficients and the deformations effect [93, 92, 26].

Combining Hooke's Law (5) with the basic relationship of dynamics:

$$\frac{\partial \sigma_{ij}}{\partial x_j} = \rho \frac{\partial^2 u_i}{\partial t^2} \qquad (8)$$

where ρ is the density and u_i is the impedance, we get the wave equation:

$$C_{ijkl} \frac{\partial^2 u_l}{\partial x_j \partial x_k} = \rho \frac{\partial^2 u_i}{\partial t^2} \qquad (9)$$

The polarized wave u0 propagates in the n direction with phase velocity V. The equation to be solved becomes:

$$C_{ijkl} n_j n_k u^0{}_l = p v^2 u_i^0 \qquad (10)$$

$\Gamma_{il} = C_{ijkl} n_j n_k$ Influential Christophel where:Γ_{il}

So we get Christofel's equation:

$$\Gamma_{il} u^0{}_l = \rho v^2 u_i^0 \qquad (11)$$

This last equation is the eigenvalue equation that gives the polarization directions of the waves and their wave velocity, respectively. This solution produces polarized directions that are not, in general, parallel or perpendicular. It can be said that the longitudinal P-waves and the S-shear quasi-waves [94].

For symmetry reasons, the number of independent coefficients of the operator Cijkl can be reduced from 81 to 21 and made into a symmetric operator of order 2 using new indices (notation de Voigt) [95]:

ij (kl)	11	22	33	23(32)	13(31)	12(21)
I(j)	1	2	3	4	5	6

The elasticity effect is given by [96]:

$$C_{ij} = \begin{pmatrix} C_{11} & \dots & C_{16} \\ \dots & \dots & \dots \\ C_{16} & \dots & C_{66} \end{pmatrix} \qquad (12)$$

The diagonal constants C_{ii} with $i \leq 3$ can be called longitudinal elastic constants.

$C_{ii}$with$i \geq 4$are called shear elastic constants.

$C_{ij}$with$i \neq j < 3$are called external diagonal constants.

The constants C_{ij} with$i \leq 3 j > 3$that measure the shear stress resulting from longitudinal compression are called mixed elastic constants [97].

For the symmetry of the cube, the three constants C_{11}, $C_{12}$and C_{44}all define constants of the same nature, where:$C_{44} = C_{55} = C_{66}$ و$C_{12} = C_{21} = C_{13} = C_{31}$ ،$C_{11} = C_{22} = C_{33}$

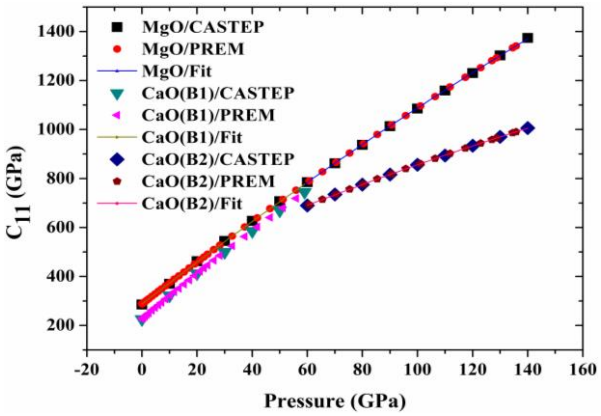

Fig 10. Changes in the values of the elastic constant C11; calculated using the CASTEP program, calculated at PREM pressures, and filtering polynomials for the MgO and CaO structures in their B1 and B2 phases with changing pressure.

It is clear from Figures (10–12) that the values of the elastic constants C11, C12, and C44 change over their respective widths: 1088.79, 180.41, and 56.32 GPa for manganese oxide, 519.39, 84.13, and 14.70 GPa for calcium oxide in phase B1, 316.45, 244.03, and 139.19 GPa for

calcium oxide in phase B2. Figures (10–12) represent the changes in all elastic constants C11, C12, and C44 with changing pressure for oxides. Within these fields, all of these constants increase with increasing pressure, except for the values of the elastic constant C44 in the second phase of calcium oxide. It can also be noted that the values of these constants for manganese oxide are larger than those for other oxides, with the exception of the values of the constants C12 and C44, respectively, in the entire range of the appearance of the second phase of calcium oxide and after a pressure of 110 GPa.

This shows that there is agreement on the values of the oxide constant is between 110 and 120 GPa. Later, this range can be determined more accurately. This increase in values occurs with varying differences. It increases for the constants C11, C12, and C44 in the range of the second phase of calcium oxide for the first two constants, as well as between the pressure values of 10 and 20 GPa for the first constant, and in the range of the first phase for the same oxide between the two pressures. 120 and 140 GPa for the latter constant. This difference is decreasing within the following areas: for the constant C11, it is between the pressures of 0 and 10 GPa and between the pressures of 20 and 59 GPa, and for the constant C44, it is between the pressures of 60 and 110 GPa. This difference is also fluctuating, as it is almost constant with respect to the constant C12 in the range of the first phase of calcium oxide.

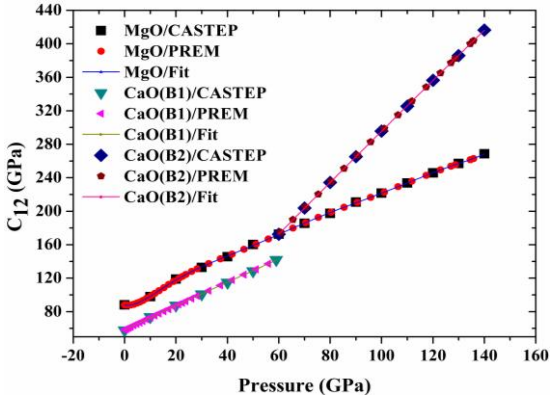

Fig 11. Changes in the values of the elastic constant C12, calculated using the CASTEP program, calculated at PREM pressures, and filtering polynomials for the MgO and CaO structures in their B1 and B2 phases with changing pressure.

When comparing the results of our calculations with the results of other studies, especially at 0 GPa, we find:

For MgO in general, we obtained lower values of elastic constants than most previous studies, with mostly good agreement. As compared to the computational studies, the agreement is better than its experimental counterpart. For example, the value of C11, C12, and C44 that we found is less than that calculated in the work of [26] by the following amounts: 5.78, 2.87, and 0.41 GPa, respectively. The difference in the values of the resulting C11 and C12 and those resulting from the values of the experimental work of [38] is estimated at 8.78 and 4.87 GPa, respectively, while

the difference for C11 and C12 compared to the experimental work of [31] is estimated at 15.81 GPa.

Always in the same order as before in the three constants, and by comparing their values for CaO resulting from our calculations with those determined in the experimental work of [57], we found that they agree with differences estimated at 4.71, 0.81, and 2.76 GPa, with their superiority only for C44. This is also the case when comparing the value of the latter and C11 resulting from our calculations with those resulting from the calculations of [81] and [70], respectively, where the difference appears with an estimated value of 1.66 and 1.50 GPa. On the contrary, the value of C12 resulting from our calculations is lower in good agreement than that resulting from the calculation of [72], with an estimated difference of 3.81 GPa.

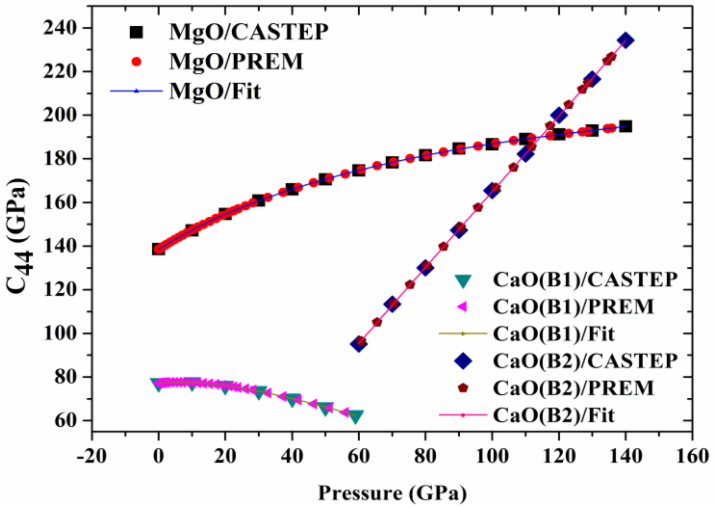

Fig 12. Changes in the values of the elastic constant C44, calculated using the CASTEP program, calculated at PREM pressures, and filtering polynomials for the MgO and CaO structures in their B1 and B2 phases with changing pressure.

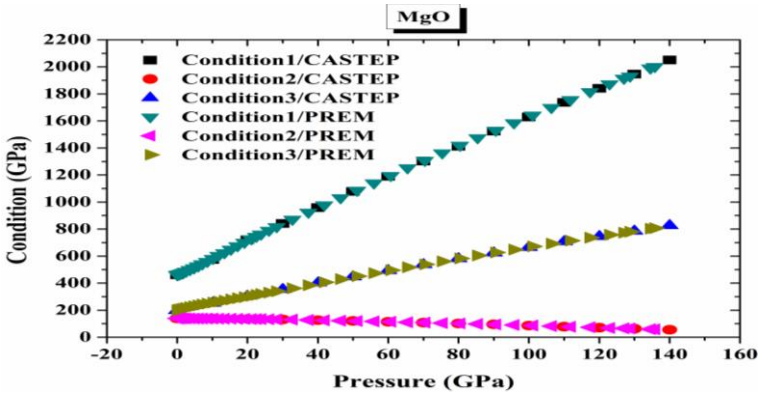

Fig 13. Changes in the values of stability conditions. Calculated using the CASTEP program, calculated at PREM pressures for the MgO structure with varying pressure

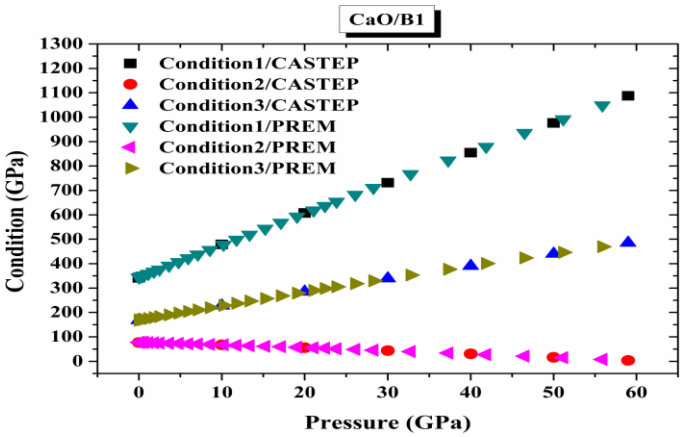

Fig 14. Changes in the values of stability conditions. Calculated using the CASTEP program, calculated at PREM pressures for the CaO structure in its B1 phase with varying pressure

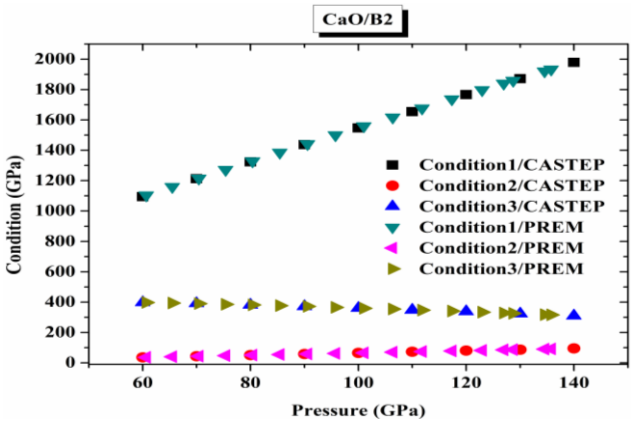

Fig 15. Changes in the values of stability conditions. Calculated using the CASTEP program, calculated at PREM pressures for the CaO structure in its B2 phase with varying pressure

So that the values of the three elastic constants can be determined at the PREM pressures, some of which are listed in Table 3, and they are those that appear at the most important boundary intervals, starting from the crust up to the boundaries of the Earth's outer core. Here we also approximated the change of these constants with changing pressure to well-fitting polynomials, whose coefficients are included in Table 2, and we found the following:

For MgO, the appropriate polynomials are second, eighth, and ninth degrees for C11, C12, and C44, respectively. As for CaO in the NaCl phase, the appropriate polynomials are second degree for C11 and C12 and sixth degree for C44, respectively. Finally, in its other phase, all appropriate polynomials, for the sake of the three constants, are of the second degree. It is also possible to benefit from this determination and easily find a more precise range than what was presented above for the possibility of matching the values of the constant C44 between the two oxides, which is between the two pressures (2471.4 km, 111.8207 GPa) and (2571.8 km, 117.3465 GPa).

Among the many benefits of calculating elastic constants, we find calculating the conditions for confirming whether the crystal is stable or not. These conditions are given in the case of the cubic crystal system by the following relations [43]:

$$Condition1 = C_{11} + 2C_{12} + P \quad (13)$$
$$Condition2 = C_{44} - P \quad (14)$$
$$Condition3 = C_{11} - C_{12} - 2P \quad (15)$$

Figures (13-15) show the changes of these conditions with changing pressure for the manganese oxide and calcium oxide phases, respectively, whether the values are calculated directly by the program or those calculated at PREM pressures.

It is clear from it that the change of the three conditions is similar between MgO and CaO in its first phase, as the first condition increased very quickly with increasing pressure compared to the second condition. With a slow decrease in the third condition, where it is almost non-existent at a pressure of 59 GPa. This confirms the tendency of two crystals towards instability, especially the calcium oxide crystal.

While in the second phase of this oxide, it is observed that the first condition maintains its rapid increase with increasing pressure compared to the third condition, while the second condition decreases slowly. This further confirms the increased stability of the oxide in this phase.

3.3.2. Bulk and shear modulus:

The bulk modulus is defined as a measure of a material's resistance to compression when external pressure is applied to that material. It is also known as the inverse relationship of compressibility. It is calculated using the following mathematical relationship [98]:

$$B = -\nu\left(\frac{\Delta P}{\Delta \nu}\right) \quad (16)$$

where ν is the volume of the material compressed to the volume Δν - ν under the influence of pressure ΔP. The sign (-) is a term that expresses that the material is subjected to compression when the pressure increases or expansion when the pressure decreases. This parameter and its unit result from a force applied to a surface, i.e., ML-1T-2. In the case of terrestrial rocks, the magnitude of this parameter is in degrees GPa 100 [43]. It is also calculated according to the following relationship [100, 99]:

$$B = \frac{1}{3}(C_{11} + 2C_{12}) \quad (17)$$

But the CASTEP program provides the values of the volumetric compression factor B directly. The shear modulus, also called the shear modulus, is symbolized by G. It is defined through experiments that do not include a change in volume but rather a change in shape that corresponds to shear, torsion, differential rotation, and so on. For simple objects such as iron, copper, tin, lead, etc., there is an empirical law established by Sutherland that states that, however, when approaching the melting point of such a material, the hardness parameter tends towards zero according to the quadratic law [101]. The fluid state is characterized by a solidity parameter of zero (G = 0). There are two ways to calculate this parameter, based on the elastic constants and the volumetric compression modulus: using the method of Voigt & Russ [103, 102], and using the Hill method [104]. This method is the one adopted in the CASTEP program and is the one

adopted in this research. The shear modulus G is calculated based on the elastic constants as follows:

$$G = \frac{G_V + G_R}{2} \quad (18)$$

$$G_V = C_{44} + 2\left(\frac{5}{C_s - C_{44}} + \frac{18(B + 2C_{44})}{5C_{44}(3B + 4C_{44})}\right) \quad (19)$$

$$G_R = C_s + 3\left(\frac{5}{C_{44} - C_s} + \frac{12(B + 2C_s)}{5C_s(3B + 4C_s)}\right) \quad (20)$$

$$C_s = \frac{C_{11} - C_{12}}{2} \quad (21)$$

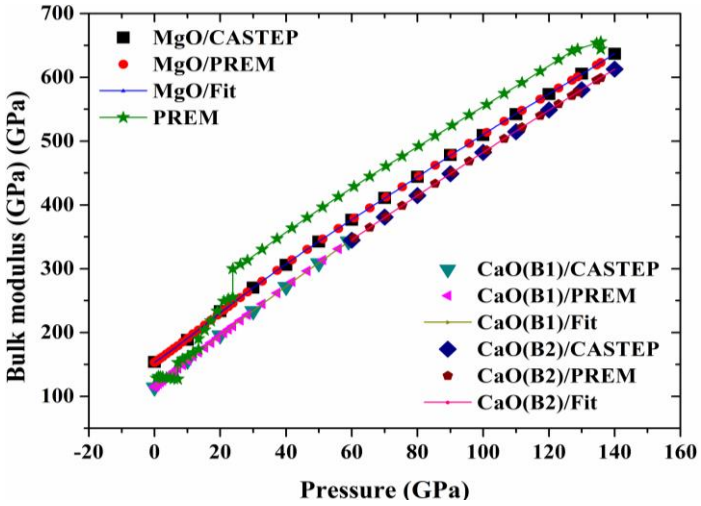

Fig 16. Changes in the values of the bulk modulus; Calculated using the CASTEP program, calculated at PREM pressures, determined from the PREM model and the appropriate filtering polynomials for the MgO and CaO structures in their B1 and B2 phases with changing pressure

After looking at the results of our calculations, part of which we display in Table 3, it can be noted that the volumetric elasticity modulus (Figure (16)) and the shear modulus (Figure (17)) change their values with the change in pressure within their width ranges, respectively: 483.2 and 179.64 GPa for manganese oxide, where the pressure changes between 0 and 140 GPa. As for calcium oxide in its first phase, where the pressure changes between 0 and 59 GPa, the widths of these bands are, respectively, 229.22 and 45 GPa. For the same oxide in its second phase, where the pressure changes between 60 and 140 GPa, the widths of these bands are always the same: 268.17 and 112.95 GPa.

From Figures (16–17), it is always clear that there is an increase in the values of both parameters with increasing pressure, but this increase occurs at varying velocitys. It turns out that the resistance of the manganese oxide material changes a little slower, with a slight difference in its values compared to that of the other oxide, which makes the small difference between them decrease with increasing pressure. The values of this difference at pressures of 0, 50, 60, and 140

GPa are, respectively, 40.05, 33.85, 31.83, and 24.02 GPa. The shear resistance values of manganese oxide are superior to those of calcium oxide, as they change faster only in the first phase of the second oxide and exactly the opposite in its second phase. This makes the difference in values between them increase in the first phase, where it takes values of 41.04 and 84.90 GPa at pressures of 0 and 50 GPa. In its second phase, the difference decreases, taking values of 75.20 and 43.66 GPa at pressures of 60 and 140 GPa.

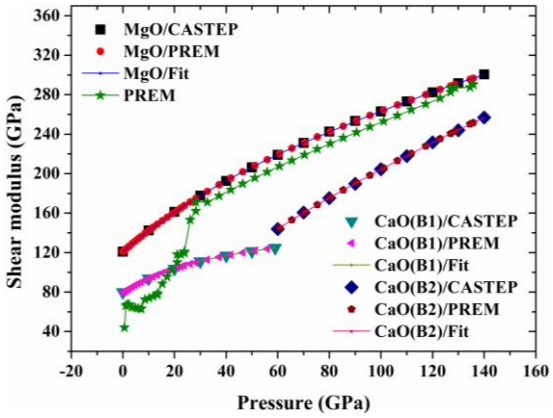

Fig 17. Changes in shear modulus values; Calculated using the CASTEP program, calculated at PREM pressures, determined from the PREM model and the appropriate filtering polynomials for the MgO and CaO structures in their B1 and B2 phases with changing pressure

The value of the bulk modulus calculated through the state function presented above is slightly higher than its value actually calculated by the program. This difference is estimated by the following amounts: 2.38 and 1.72 GPa, especially for manganese oxide and calcium oxide. Therefore, comparing the values of this parameter at zero pressure resulting from our study with the rest of the studies remains the same as the previous comparison.

As for comparing the values of the shear modulus and always at zero pressure, the results of our calculations are largely consistent with previous studies, whether experimental or computational, for both oxides. The values resulting from our study are lower than those determined in both the experimental study of [68] regarding calcium oxide, with an estimated difference of 1.24 GPa, and the two computational studies [26] and [58] regarding the same oxide and the second oxide, respectively. It is respectively also estimated at 0.61 and 3.74 GPa. While the value of this parameter resulting from our calculations for manganese oxide is higher than that published in the experimental work of [41], with a difference estimated at 0.89 GPa.

From Figure (16) it is noted that; The compressive resistance values of the Earth's material are higher than those of manganese oxide at the end of the upper mantle region at the pressure limit of 20 GPa, with a decreasing difference at the beginning of the Earth's lower mantle. While this resistance of the Earth material is higher than that of calcium oxide starting at a pressure of 10 GPa, before that the picture is not completely clear due to the presence of multiple layers.

As for the shear resistance of the Earth's material, from Figure (17), it is clear that it is always less than that of manganese oxide, but with a very weak difference over the entire Earth's lower mantle, decreasing at the beginning of the outskirts of the middle of the Earth's upper mantle, that is, starting from a pressure of 10 GPa. As for the second oxide, this resistance and its characteristic are less than that of the earth's matter throughout the entire lower earth's mantle, where on its borders their values match. This occurs with an oscillating difference in the other two ranges, and increases based on the clamping pressure until the end of the first phase of this oxide and decreases in its second phase.

As shown in Table 3, we were able to determine the values of the elasticity parameters at the boundary depths between the most important internal Earth layers, especially up to the outer Earth core. This happened after we were able to determine the values of the two parameters at pressures in the PREM model, by approximating their change with pressure changes to appropriate polynomials. These are the polynomials whose parameters were recorded in Table 2 as shown, where we found that polynomials of the fourth degree are the most appropriate for changing the shear modulus for both oxides, in addition to changing the bulk modulus in the case of calcium oxide when it stabilizes in the first phase. As for In its second phase, the change in this parameter takes the form of a second-degree polynomial, while for manganese oxide, the change in this parameter always takes the form of a sixth-degree polynomial.

Despite this improvement in the results after this choice of polynomials that change the parameters with changes in pressure, nothing significant was presented about the value of the development of the difference between the two oxides.

However, it has become possible to compare the results of our study with the values of the two parameters with those of the Earth matter with greater accuracy, if it is calculated based on their relationship to the longitudinal wave velocities Vp and the transverse wave velocities Vs and the density of the material ρ, the values of which are available in the work of [08]. This is according to the following relationships:

$$G = \rho . V_s^2 \qquad (22)$$

$$B = \rho . V_p^2 - \frac{4}{3}\rho . V_s^2 \qquad (23)$$

Thus, we obtain the rest of the curves in Figures (16 and 17), from which it is noted that:

Regarding the resistance of the Earth material to compression, it applies to its counterpart of manganese oxide when the pressure is between the two values (500 km, 17.1311 GPa) and (550 km, 19.0703 GPa), where the difference is very small and is estimated at 1.22 and 6.10 GPa, respectively. It decreases in seven areas, most of which are between the crust and the upper mantle, and only two areas in the Earth's lower mantle. The smallest difference appears at the pressure (500 km, 17.1311 GPa) by 6.10 GPa, while the highest difference appears at the pressure (22.34 km, 0.604 GPa), and its amount is 80 GPa. As for shear resistance, the difference between its values for the Earth's material and its counterpart for this oxide is decreasing in five ranges, as the

decrease only appears in a single range in the Earth's lower mantle. The smallest difference appears at the pressure (771 km, 28.2928 GPa), and its value is 3.81 GPa, while the highest appears at the pressure (15 km, 0.3364 GPa), which is estimated at 95.40 GPa.

The resistance of the earth material to compression is less than that of calcium oxide from the surface of the earth's crust until pressure (24.4 km, 0.604 GPa), after which the first impact occurs in their values. This superiority also occurs between the two pressures (115 km, 3.6183 GPa) and (220 km, 7.1108 GPa), as the lowest value of the difference appears at the first pressure, which is estimated at 0.13 GPa. What is the highest difference ever? It appears at pressure (670 km, 28.8342 GPa), that is, at the beginning of the Earth's lower mantle, where its value is estimated at 89.73 GPa. This difference is decreasing in seven different ranges, most of which are between the Earth's crust and the Earth's upper mantle, and the longest of them is in the Earth's lower mantle. The same applies to the difference between the values of the shear strength of the Earth material and that of this oxide, as most of the areas of decrease are in the same two regions, and the longest field of decrease is in the same region as well. However, the number of these fields is one less than previously. The smallest amount is estimated at 3.88 GPa and appears at pressure (450 km, 15.2251 GPa). Between this pressure and (500 km, 17.1311 GPa), a match occurs in the value of shear resistance between the two materials, that is, at the end of the Earth's upper mantle. The highest value of this difference is at the end of the first phase of this oxide, that is, at pressure (1371 km, 55.8991 GPa), so the value of this difference is 83.85 GPa.

3.3.3. Wave velocities:

The relationship by which both the longitudinal and transverse wave velocities are calculated can be deduced using the aforementioned relationships (22) and (23). The sound compression wave velocity can also be deduced from knowing the values of density and bulk modulus, which are written as follows:

$$V_{\varphi}^2 = \frac{B}{\rho} \qquad (24)$$

It can also be calculated based on knowing the values of the longitudinal and transverse wave velocities, through the following relationship:

$$V_{\varphi}^2 = V_p^2 - \frac{4}{3}V_s^2 \qquad (25)$$

Figures (18-20) change the velocities of longitudinal and transverse waves and sound pressure with changes in pressure, which, according to the values of Table 3, also change in their areas of width, respectively; 3.73, 1.72 and 3.17 km/s for manganese oxide, while for calcium oxide in its first phase it is; 1.15, 0.42 and 1.06 km/s and finally, for its other phase, it is: 2.40, 1.21 and 1.95 km/s.

The values of these velocities always increase with increasing pressure in a non-linear manner. The change is fastest in the case of calcium oxide in its second phase and slowest in the case of its first phase. In the latter case and in the case of manganese oxide, the intensity of the deceleration

increases at the highest pressures. The difference between the values of the three oxide velocities within the range of the first phase of calcium oxide is increasing, as its values at zero pressure are always the same, respectively: 1.95, 1.05, and 1.53 km/s, and its value at 50 GPa is 3.05, 1.66, and 2.38 km/s. While this difference is decreasing within the second field of calcium oxide, where its values at a pressure of 60 GPa are always the same, respectively, 3.19, 1.71, and 2.51 km/s, and its value at a pressure of 140 GPa is 2.56, 1.07, and 1.64 km/s.

At zero pressure, for manganese oxide and for the value of the longitudinal wave velocity, our calculation result agrees well with that result presented in the work of [26], while it also agrees well with the experimental one with an estimated difference of 1.61 km/s and determined in the work of [31]. As for the value of the transverse wave velocity, our calculation result matches to a large extent that resulting from the calculation in [43], while it agrees poorly with the experimental one, with a difference estimated at 0.16 km/s and determined in the work of [31]. Finally, as for the velocity of the acoustic compression wave, it is the least studied in most previous studies, and it has not even been determined experimentally. Mathematically, it was only indicated through the work of [26], where we found that the value of our calculation is less consistent with superiority, with the difference estimated at 2.26 km/s.

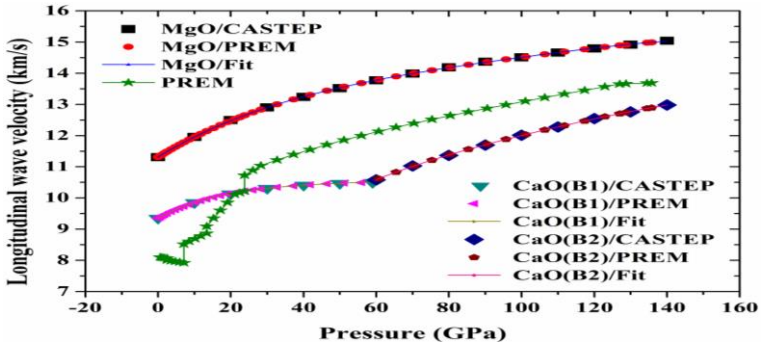

Fig 18. Changes in longitudinal wave velocity values; Calculated using the CASTEP program, calculated at PREM pressures, determined from the PREM model and the appropriate filtering polynomials for the MgO and CaO structures in their B1 and B2 phases with changing pressure

For calcium oxide at zero pressure, it is unfortunate that the calculation or measurement of the acoustic compression wave velocity value was not taken into account in previous studies. While it appears that the values of the two wave velocities, whether longitudinal or transverse, calculated in the work of [59] converge greatly based on the results of our study, this convergence is almost identical for the first wave. The values of our calculations for the velocity of the first wave are in great agreement with a decrease in that resulting experimentally in the work of [68], with an estimated difference of 1.6 km/s, while the opposite is for the velocity of the second wave, where the agreement is also good, with the result of the experimental work of [71] being superior by an estimated difference. At 0.1 km/s.

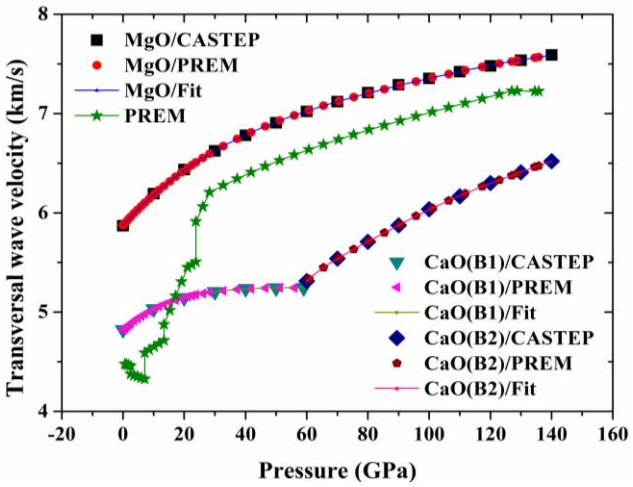

Fig 19. Changes in the values of the transverse wave velocity; Calculated using the CASTEP program, calculated at PREM pressures, determined from the PREM model and the appropriate filtering polynomials for the MgO and CaO structures in their B1 and B2 phases with changing pressure

Studying the velocity of these waves is considered the second reading in seismic observations, so it is necessary to determine their values at PREM pressures so that the comparison between them and those available in the same model is accurate, i.e., each value. If the velocity of the waves in this model represents their velocity in the Earth's matter, in other words, this comparison is based on the material content of the Earth's interior.

From the same shapes, it is always noticeable that the velocities of the three waves in the PREM model change within the ranges of 5.77, 2.90, and 4.71 km/s, respectively. These velocities are always increasing, starting from a pressure of 7.1108 GPa, that is, starting from an estimated depth of 220 km. The values of these velocities for this model fall between the values of the two oxides. This is the beginning of certain pressures, which are mostly from the beginning of the Earth's lower mantle. In addition to this, it appears that the values of longitudinal wave velocities and acoustic pressure converge to those of calcium oxide in its second phase, especially those of the latter, where the convergence is to a large extent. While the values of the transverse wave velocities are more similar to those of manganese oxide,

After calculating, we found that the degrees of the polynomials most suitable for changing the values of these velocities with changes in pressure are: The fourth is for the longitudinal wave in all cases, and the fifth, fourth, and sixth are for manganese oxide and calcium oxide in their first and second phases, respectively.

This result enables us to determine the values of these velocities at PREM pressures, although it is not considered significant, because it does not add anything to the difference between their values for the two oxides except to identify the accuracy of this difference, especially at important interruptions in the Earth's interior up to the borders of the outer core. But it is considered a very

important result because it enables us to determine the changes in the difference between the values of the velocities of this model and those of the two oxides, where:

Table 3. The values of the studied parameters at the pressures of the main sections of the Earth's interior up to the Gothenburg area, in addition to their values at the pressures of 59, 60, and 140 GPa for both MgO and CaO

		Crust		Uppermantle		Lowermantle				
Depth (Km)		0	80	80	670	670	/	/	2891	/
Pressure (GPa)		0	2,4539	2,4546	23,8334	23,8342	59	60	135,7509	140
Final Enthalpy (keV)	MgO	-2.13	-2.13	-2.13	-2.13	-2.13	/	-2.123	-2.12	-2.12
	CaO	-1.44	-1.44	-1.44	-1.44	-1.44	-1.43	-1.44	-1.43	-1.43
Latticeparameters (A)	MgO	3	2.98	2.98	2.88	2.88	/	2.73	2.63	2.63
	CaO	3.37	3.35	3.35	3.21	3.21	3.07	2.63	2.49	2.49
Currentcell volume (A^3)	MgO	19.08	18.78	18.78	16.92	16.92	/	14.35	12.92	12.83
	CaO	27.10	26.57	26.57	23.34	23.34	20.52	18.27	15.52	15.41
V/V_0	MgO	1	0.98	0.98	0.89	0.89	/	0.79	0.68	0.67
	CaO	1	0.98	0.98	0.89	0.89	0.76	0.67	0.57	0.57
Density (g/cm^3)	MgO	3.51	3.56	3.56	3.95	3.95	/	4.44	5.18	5.22
	CaO	3.44	3.51	3.51	3.99	3.99	4.54	5.10	6.00	6.04
	PREM	1,02	3,38	3,38	3,99	4,38	/	/	5,57	/
C_{11} (GPa)	MgO	285.21	308.71	308.71	490.72	490.72	/	785.09	1341.44	1374.00
	CaO	225.71	250.06	250.07	445.58	445.58	745.09	689.44	990.70	1005.88
C_{12} (GPa)	MgO	88.13	88.08	88.08	124.39	124.39	/	172.45	262.98	268.53
	CaO	57.81	61.97	61.97	92.47	92.47	141.95	172.53	403.61	416.56
C_{44} (GPa)	MgO	138.59	140.87	140.87	157.12	157.12	/	174.66	194.08	194.91
	CaO	77.24	77.49	77.49	75.21	75.21	62.54	95.18	226.89	234.37
Bulkmodulus (GPa)	MgO	153.82	161.93	161.93	245.98	245.98	/	376.67	623.13	637.02

	CaO	113.78	124.67	124.67	210.17	210.17	343	344.83	599.31	613.00
	PREM	2.14	130.48	129.86	255.82	10,73	/	/	300.3	/
Shearmodulus (GPa)	MgO	120.89	126.55	126.55	167.61	167.61	/	219.12	296.73	300.53
	CaO	79.86	83.66	83.66	106.77	106.77	124.87	143.93	251.61	256.87
	PREM	0	67.23	64.84	120.7	152.99	/	/	291.16	/
Velocity of longitudinal wave (km/s)	MgO	11.31	11.49	11.49	12.65	12.65	/	13.77	14.99	15.04
	CaO	9.35	9.50	9.50	10.22	10.22	10.50	10.58	12.90	12.98
	PREM	1,45	8,07	8	10,22	10,73	/	/	13,69	/
Velocity of transversal wave (km/s)	MgO	5.87	5.96	5.96	6.51	6.51	/	7.02	7.57	7.59
	CaO	4.82	4.88	4.88	5.17	5.17	5.25	5.13	6.47	6.52
	PREM	0	4,46	4,38	5,5	5,91	/	/	7,23	/
Velocity of bulk sound wave (km/s)	MgO	9.05	9.19	9.19	10.18	10.18	/	11.13	12.18	12.22
	CaO	7.52	7.64	7.64	8.29	8.29	8.58	8.62	10.50	10.58
	PREM	1,45	6,21	6,2	8	8,28	/	/	10,85	/

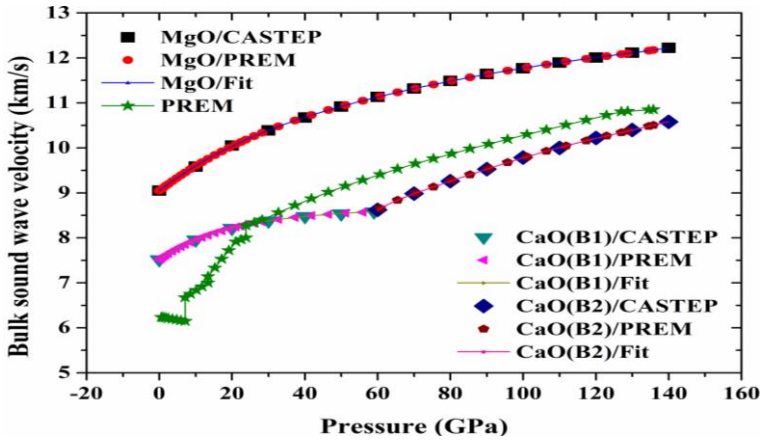

Fig 20. Changes in the velocity values of the acoustic compression wave. Calculated using the CASTEP program, calculated at PREM pressures, determined from the PREM model and the appropriate filtering polynomials for the MgO and CaO structures in their B1 and B2 phases with changing pressure

Between its values and the values of manganese oxide for the velocities of the longitudinal wave and the acoustic compression wave, there is an increasing difference in eight areas, most of which are between the crust and the upper mantle. Three of the areas are identical, especially in the first area in its entirety, up to the pressure or depth (24.4 km, 0.604 GPa) in the second area, while this difference is increasing in one area, starting from the pressure or depth (2741 km, 126.9741 GPa), that is, at the end of Earth's lower mantle. As for the transverse velocity of sound, this difference is increasing in only seven areas, only two of which are in the Earth's lower mantle. In addition to the previously mentioned field, which is located at the end of this mantle, the second field is located between (971 km, 37.2852 GPa) and (1171 km, 46.4882 GPa). The smallest difference always appears at pressure or depth (2741 km, 126.9741 GPa), where its values are 1.24 km for the longitudinal wave velocity, 0.30 km for the transverse wave velocity, and 1.28 km for the acoustic compression wave velocity. While the highest difference always appears at pressure or depth (3 km, 0.0299 GPa), its values are 9.87 km for the longitudinal wave velocity, 5.88 km for the transverse wave velocity, and 7.60 km for the acoustic compression wave velocity.

Between the model values and the calcium oxide values for longitudinal and transverse wave velocities and acoustic pressure, the difference increases in five areas, most of which are also located between the crust and the upper mantle. Four of them are identical, especially in the entire first region, and even the pressure or depth (220 km, 7.1108 GPa) is located in the second region. While this difference is increasing in a single range for the velocities of the first two waves and in the same sequence based on the pressure or depth (670 km, 23.8334 GPa) and (500 km, 17.1311 GPa), which are also located in the second region, But for the velocity of the third wave, the field starts from the pressure or depth (721 km, 26.0783 GPa), which is located in the Earth's lower mantle. This field ends for the velocity of the first and third waves at the beginning of the second phase of calcium oxide, that is, at the pressure or depth (1471 km, 60.683 GPa), and for the velocity of the second wave, it ends at the end of the first phase of calcium oxide, that is, at the pressure or depth (1371 km, 55.8991 GPa). This difference has its maximum value at pressure or depth (3 km, 0.0299 GPa), where its values are always 7.90, 4.82, and 6.07 km, respectively. While the values of the pressures or depths at which the minimum value of this difference appears vary, as for the velocities of the first two waves, it is located at the end of the Earth's upper mantle, that is, at 670 km, 23.8334 GPa, and its values are respectively estimated at 0.00095 and 0.33 km, as for the velocity of the third wave. The smallest difference appears at pressure or depth (721 km, 26.0783 GPa), that is, approximately at the beginning of the Earth's lower mantle. The value of this difference is 0.013 km.

This result also enables determining the pressures or depths at which the values of the three velocities can match those of the PREM model, which were previously mentioned without being specified with such precision. Taking the same previous wave arrangement, these locations are limited to the bands that begin with (635 km, 22.4364 GPa), (450 km, 15.2251 GPa), and (670

km, 23.8334 GPa), and end with (670 km, 23.8334 GPa). (500 km, 17.1311 GPa) and (670 km, 23.8342 GPa).

5. Conclusion:

Using the PBEsol function of the GGA approximation DFT method, which appeared in 2008, along with some simple mathematical methods, we calculated some parameters of the structural and elastic properties of both manganese and calcium oxide with varying pressure in a range from 0 to 140 GPa. We found:

Confirmation of the stability of manganese oxide in its first phase, B1, in this field, while we confirmed the occurrence of a phase transition from phase B1 towards the second phase, B2, of calcium oxide at a very precise pressure, estimated at 59.2 GPa, consistent with computational and other experimental studies.The results of our calculations for all the parameters studied were also consistent with previous studies, whether these works were experimental or computational as well.We were able to choose polynomials to vary these parameters with changes in pressure by calculating the constants of these functions.This choice enabled us to determine the values of the parameters at PREM pressures, which represents the earth's material. This choice determines the depths at which the values of the two oxides converge or apply, on the one hand, and on the other hand, between each oxide and the Earth substance. In the future, it is possible to suggest a number of research directions that always fall within this scope, which are:

Investing the results of this study to calculate other parameters, such as Young's modulus, Poisson's constant, etc., as elastic constants. The study can also be completed to include other properties related to the parameters studied here, such as thermodynamic properties. The same study steps can be repeated on many other subjects.

References

[1] Bullen, K. E., & Bolt, B. A. (1985). *An introduction to the theory of seismology*.Cambridge universitypress.

[2] Poirier, J. P. (2000). *Introduction to the Physics of the Earth's Interior*.Cambridge UniversityPress.

[3] Shearer, P. M. (2009). Introduction to Seismology, Cambridge University Press.

[4] Jackson, I. (Ed.). (2000). *The Earth's mantle: composition, structure, and evolution*. Cambridge UniversityPress.

[5] Radovic, M., Lara-Curzio, E., &Riester, L. (2004). Comparison of different experimental techniques for determination of elastic properties of solids. *Materials Science and Engineering: A*, *368*(1-2), 56-70.

[6] Wang, S. F., Hsu, Y. F., Pu, J. C., Sung, J. C., &Hwa, L. G. (2004). Determination of acoustic wave velocities and elastic properties for diamond and other hard materials. *Materials Chemistry and Physics*, *85*(2-3), 432-437.

[7] Stein, C. A. (1991). The solid earth: an introduction to global geophysics.

[8] Dziewonski, A. M., & Anderson, D. L. (1981). Preliminary reference Earth model. *Physics of the earth and planetary interiors*, *25*(4), 297-356.

[9] Kennett, B. L. N. (2006). On seismological reference models and the perceived nature of heterogeneity. *Physics of the Earth and PlanetaryInteriors*, *159*(3-4), 129-139.

[10] Völgyesi, L., & Moser, M. (1985). The inner structure of the Moon. *PeriodicaPolytechnica Chemical Engineering*, *29*(1), 59-70.

[11] Wyckoff, R. W. G. (1963). Crystal structure descriptions. *New York: Wiley*, *1*, 28.

[12] Weaver, C. W., & Paterson, M. S. (1969). Deformation of cube-oriented MgO crystals under pressure. *Journal of the American Ceramic Society*, *52*(6), 293-302.
[13] Paterson, M. S., & Weaver, C. W. (1970). Deformation of polycrystalline MgO under pressure. *Journal of the American Ceramic Society*, *53*(8), 463-471.
[14] Hazen, R. M. (1976). Effects of temperature and pressure on the cell dimension and X-ray temperature factors of periclase. *American Mineralogist*, *61*(3-4), 266-271.
[15] Vassiliou, M. S., & Ahrens, T. J. (1981). Hugoniot equation of state of periclase to 200 GPa. *GeophysicalResearchLetters*, *8*(7), 729-732.
[16] Bukowinski, M. S. T. (1985). First principles equations of state of MgO and CaO. *Geophysical Research Letters*, *12*(8), 536-539.
[17] Sumino, Y., Anderson, O. L., & Suzuki, I. (1988). Temperature coefficients of elastic constants of single crystal MgO between 80 and 1,300 K. *Elastic Properties and Equations of State*, *26*, 503-512.
[18] Meade, C., &Jeanloz, R. (1988). Yield strength of MgO to 40 GPa. *Journal of Geophysical Research: Solid Earth*, *93*(B4), 3261-3269.
[19] Isaak, D. G., Anderson, O. L., &Goto, T. (1989). Measured elastic moduli of single-crystal MgO up to 1800 K. *Physics and Chemistry of Minerals*, *16*, 704-713.
[20] Yoneda, A. (1990). Pressure derivatives of elastic constants of single crystal MgO and MgAl2O4. *Journal of Physics of the Earth*, *38*(1), 19-55.
[21] Isaak, D. G., Cohen, R. E., &Mehl, M. J. (1990). Calculated elastic and thermal properties of MgO at high pressures and temperatures. *Journal of Geophysical Research: Solid Earth*, *95*(B5), 7055-7067.
[22] Saxena, S. K., & Zhang, J. (1990). Thermochemical and pressure-volume-temperature systematics of data on solids, examples: tungsten and MgO. *Physics and Chemistry of Minerals*, *17*(1), 45-51.
[23] Anderson, O. L., &Zou, K. (1990). Thermodynamic functions and properties of MgO at high compression and high temperature. *Journal of Physical and Chemical Reference Data*, *19*(1), 69-83.
[24] Chopelas, A. (1992). Sound velocities of MgO to very high compression. *Earth and planetary science letters*, *114*(1), 185-192.
[25] Duffy, T. S., Hemley, R. J., & Mao, H. K. (1995). Equation of state and shear strength at multimegabar pressures: Magnesium oxide to 227 GPa. *PhysicalReviewLetters*, *74*(8), 1371.
[26] Karki, B. B., Stixrude, L., Clark, S. J., Warren, M. C., Ackland, G. J., & Crain, J. (1997). Structure and elasticity of MgO at high pressure. *American Mineralogist*, *82*(1-2), 51-60.
[27] Chen, G., Liebermann, R. C., & Weidner, D. J. (1998). Elasticity of single-crystal MgO to 8 Gigapascals and 1600 Kelvin. *Science*, *280*(5371), 1913-1916.
[28] Utsumi, W., Weidner, D. J., & Liebermann, R. C. (1998). Volume measurement of MgO at high pressures and high temperatures. *GeophysicalMonograph-American Geophysical Union*, *101*, 327-334.
[29] Sinogeikin, S. V., & Bass, J. D. (1999). Single-crystal elasticity of MgO at high pressure. *PhysicalReview B*, *59*(22), R14141.
[30] Karki, B. B., Wentzcovitch, R. D., De Gironcoli, S., &Baroni, S. (1999). First-principles determination of elastic anisotropy and wave velocities of MgO at lower mantle conditions. *Science*, *286*(5445), 1705-1707.
[31] Sinogeikin, S. V., & Bass, J. D. (2000). Single-crystal elasticity of pyrope and MgO to 20 GPa by Brillouin scattering in the diamond cell. *Physics of the Earth and PlanetaryInteriors*, *120*(1-2), 43-62.
[32] Zha, C. S., Mao, H. K., &Hemley, R. J. (2000). Elasticity of MgO and a primary pressure scale to 55 GPa. *Proceedings of the National Academy of Sciences*, *97*(25), 13494-13499.
[33] Karki, B. B., Wentzcovitch, R. M., De Gironcoli, S., &Baroni, S. (2000). High-pressure lattice dynamics and thermoelasticity of MgO. *Physical Review B*, *61*(13), 8793.
[34] Zhang, J. (2000). Effect of pressure on the thermal expansion of MgO up to 8.2 GPa. *Physics and Chemistry of Minerals*, *27*, 145-148.
[35] Merkel, S., Wenk, H. R., Shu, J., Shen, G., Gillet, P., Mao, H. K., &Hemley, R. J. (2002). Deformation of polycrystalline MgO at pressures of the lower mantle. *Journal of Geophysical Research: Solid Earth*, *107*(B11), ECV-3.
[36] Oganov, A. R., Gillan, M. J., & Price, G. D. (2003). Ab initio lattice dynamics and structural stability of MgO. *The Journal of chemical physics*, *118*(22), 10174-10182.
[37] Webb, S., & Jackson, I. (2003). Anelasticity and microcreep in polycrystalline MgO at high temperature: an exploratory study. *Physics and Chemistry of Minerals*, *30*, 157-166.

[38] Sun, X., Chen, Q., Chu, Y., & Wang, C. (2005). Properties of MgO at high pressures: Shell-model molecular dynamics simulation. *Physica B: Condensed Matter*, *370*(1-4), 186-194.
[39] Lu, L. Y., Cheng, Y., Chen, X. R., & Zhu, J. (2005). Thermodynamic properties of MgO under high pressure from first-principles calculations. *Physica B: Condensed Matter*, *370*(1-4), 236-242.
[40] Zhao, J. Z., Lu, L. Y., Chen, X. R., &Bai, Y. L. (2007). First-principles calculations for elastic properties of the rocksalt structure MgO. *Physica B: Condensed Matter*, *387*(1-2), 245-249.
[41] Dorogokupets, P. I., &Oganov, A. R. (2007). Ruby, metals, and MgO as alternative pressure scales: A semiempirical description of shock-wave, ultrasonic, x-ray, and thermochemical data at high temperatures and pressures. *Physical Review B*, *75*(2), 024115.
[42] Wu, Z., Wentzcovitch, R. M., Umemoto, K., Li, B., Hirose, K., &Zheng, J. C. (2008). Pressure-volume-temperature relations in MgO: An ultrahigh pressure-temperature scale for planetary sciences applications. *Journal of Geophysical Research: Solid Earth*, *113*(B6).
[43] Hachemi, A., Saoudi, A., Louail, L., Maouche, D., &Bouguerra, A. (2009). Elasticity of the B2 phase and the effect of the B1–B2 phase transition on the elasticity of MgO. *Phase Transitions*, *82*(1), 87-97.
[44] Scanavino, I., Belousov, R., &Prencipe, M. (2012). Ab initio quantum-mechanical study of the effects of the inclusion of iron on thermoelastic and thermodynamic properties of periclase (MgO). *Physics and Chemistry of Minerals*, *39*, 649-663.
[45] Cebulla, D., &Redmer, R. (2014). Ab initio simulations of MgO under extreme conditions. *Physical Review B*, *89*(13), 134107.
[46]Gour, A., Shareef M, F., & Singh, S. (2015). Pressure-induced phase transition and structural behavior of MgO at high temperatures: a model study. *Phase Transitions*, *88*(1), 1-15.
[47] Sokolova, T. S., Dorogokupets, P. I., Dymshits, A. M., Danilov, B. S., &Litasov, K. D. (2016). Microsoft excel spreadsheets for calculation of P–V–T relations and thermodynamic properties from equations of state of MgO, diamond and nine metals as pressure markers in high-pressure and high-temperature experiments. *Computers &Geosciences*, *94*, 162-169.
[48] Belmonte, D. (2017). First principles thermodynamics of minerals at HP–HT conditions: MgO as a prototypical material. *Minerals*, *7*(10), 183.
[49] Miao, Y., Li, H., Wang, H., He, K., & Wang, Q. (2018). First principles and Debye model study of the thermodynamic, electronic and optical properties of MgO under high-temperature and pressure. *International Journal of Modern Physics B*, *32*(05), 1850047.
[50] Gu, J., Wang, C., Sun, B., Zhang, W., & Liu, D. (2019). High-pressure third-order elastic constants of MgO single crystal: First-principles investigation. *ZeitschriftfürNaturforschung A*, *74*(5), 447-456.
[51] Fan, D., Fu, S., Yang, J., Tkachev, S. N., Prakapenka, V. B., & Lin, J. F. (2019). Elasticity of single-crystal periclase at high pressure and temperature: The effect of iron on the elasticity and seismic parameters of ferropericlase in the lower mantle. *American Mineralogist*, *104*(2), 262-275.
[52] Hieu, H. K., Hong, N. T., &Khoa, D. Q. (2019). Melting temperature and shear modulus of MgO under high pressure. *Journal of the Physical Society of Japan*, *88*(10), 105002.
[53] Jeanloz, R., Ahrens, T. J., Mao, H. K., & Bell, P. M. (1979). B1-B2 transition in calcium oxide from shock-wave and diamond-cell experiments. *Science*, *206*(4420), 829-830.
[54] Mammone, J. F., Mao, H. K., & Bell, P. M. (1981). Equations of state of CaO under static pressure conditions. *GeophysicalResearchLetters*, *8*(2), 140-142.
[55] Richet, P., Mao, H. K., & Bell, P. M. (1988). Static compression and equation of state of CaO to 1.35 Mbar. *Journal of GeophysicalResearch: Solid Earth*, *93*(B12), 15279-15288.
[56] Oda, H., Anderson, O. L., Isaak, D. G., & Suzuki, I. (1992). Measurement of elastic properties of single-crystal CaO up to 1200 K. *Physics and Chemistry of Minerals*, *19*, 96-105.
[57] Zhang, H., &Bukowinski, M. S. T. (1991). Modified potential-induced-breathing model of potentials between close-shell ions. *PhysicalReview B*, *44*(6), 2495.
[58] Karki, B. B., & Crain, J. (1998). Structure and elasticity of CaO at high pressure. *Journal of GeophysicalResearch: Solid Earth*, *103*(B6), 12405-12411.
[59] Louail, L., Krachni, O., Bouguerra, A., & Sahraoui, F. A. (2006). Effect of pressure on structural and elastic properties of alkaline-earth oxide CaO. *MaterialsLetters*, *60*(25-26), 3153-3155.
[60] Bhardwaj, P., & Singh, S. (2010). Role of temperature in the numerical analysis of CaO under high pressure. *Open Chemistry*, *8*(1), 126-133.

[61] Kürkçü, C., Merdan, Z., &Yamçıçıer, Ç. (2018). Structural phase transition and electronic properties of CaO under high pressure. *MaterialsResearch Express*, *5*(12), 125903.
[62] Vyas, P., Bhatt, N. K., &Vyas, P. R. (2021, August). Study of temperature dependent elastic properties of CaO.In *AIP ConferenceProceedings* (Vol. 2352, No. 1). AIP Publishing.
[63] Cohen, A. J., & Gordon, R. G. (1976). Modified electron-gas study of the stability, elastic properties, and high-pressure behavior of MgO and CaO crystals. *PhysicalReview B*, *14*(10), 4593.
[64] Bukowinski, M. S. T. (1985). First principles equations of state of MgO and CaO. *Geophysical Research Letters*, *12*(8), 536-539.
[65] Mehl, M. J., Cohen, R. E., &Krakauer, H. (1988). Linearized augmented plane wave electronic structure calculations for MgO and CaO. *Journal of GeophysicalResearch: Solid Earth*, *93*(B7), 8009-8022.
[66] Wu, X., Liu, L., Li, W., Wang, R., & Liu, Q. (2014). Effect of temperature on elastic constants, generalized stacking fault energy and dislocation cores in MgO and CaO. *Computational Condensed Matter*, *1*, 38-44.
[67] Liu, M., & Liu, L. G. (1987). Bulk moduli of wüstite and periclase: a comparative study. *Physics of the earth and planetaryinteriors*, *45*(3), 273-279.
[68] Son, P. R., and R. A. Barrels, CaO and SrO single crystal elastic constants and thief
pressureerivatives, J. Phys. Chem. Solids,, 819-828, 1972.
[69] Labidi, S., Zeroual, J., Labidi, M., Klaa, K., & Bensalem, R. (2017). Structural electronic and optical properties of MgO, CaO and SrO binary compounds: comparison study. *Solid State Phenomena*, *257*, 123-126.
[70] Cinthia, A. J., Priyanga, G. S., Rajeswarapalanichamy, R., &Iyakutti, K. (2015). Structural, electronic and mechanical properties of alkaline earth metal oxides MO (M= Be, Mg, Ca, Sr, Ba). *Journal of Physics and Chemistry of Solids*, *79*, 23-42.
[71] Mehl, M. J., Hemley, R. J., & Boyer, L. L. (1986). Potential-induced breathing model for the elastic moduli and high-pressure behavior of the cubic alkaline-earth oxides. *Physical Review B*, *33*(12), 8685.
[72] Baltache, H., Khenata, R., Sahnoun, M., Driz, M., Abbar, B., &Bouhafs, B. (2004). Full
potential calculation of structural, electronic and elastic properties of alkaline earth oxides
MgO, CaO and SrO. Physica B: Condensed Matter, 344(1-4), 334-342.
[73] Pandey, V., Gupta, S., Rathi, S. K., &Goyal, S. C. (2010). Elastic properties of alkaline earth oxides under high pressure. *Phase Transitions*, *83*(12), 1059-1071.
[74] Bhardwaj, P., Singh, S., & Gaur, N. K. (2009). Structural, elastic and thermophysical properties of divalent metal oxides with NaCl structure. *MaterialsResearch Bulletin*, *44*(6), 1366-1374.
[75] Lin, J. F., Heinz, D. L., Mao, H. K., Hemley, R. J., Devine, J. M., Li, J., &Shen, G. (2003). Stability of magnesiowüstite in Earth's lower mantle. *Proceedings of the National Academy of Sciences*, *100*(8), 4405-4408.
[76] Fei, Y. (1999). Effects of temperature and composition on the bulk modulus of (Mg, Fe) O. *American Mineralogist*, *84*(3), 272-276.
[77] Leonov, I., Ponomareva, A. V., Nazarov, R., &Abrikosov, I. A. (2017). Pressure-induced spin-state transition of iron in magnesiowüstite (Fe, Mg) O. *Physical Review B*, *96*(7), 075136.
[78] Holmström, E., Stixrude, L., Scipioni, R., & Foster, A. S. (2018). Electronic conductivity of solid and liquid (Mg, Fe) O computed from first principles. *Earth and Planetary Science Letters*, *490*, 11-19.
[79] Chopelas, A. (1996). Thermal expansivity of lower mantle phases MgO and MgSiO3 perovskite at high pressure derived from vibrational spectroscopy. *Physics of the Earth and PlanetaryInteriors*, *98*(1-2), 3-15.
[80] Stixrude, L. (1998). Elastic constants and anisotropy of MgSiO3 perovskite, periclase, and SiO2 at high pressure. *The Core-MantleBoundaryRegion*, *28*, 83-96.
[81] Guo, Y. D., Cheng, X. L., Zhou, L. P., Liu, Z. J., & Yang, X. D. (2006). First-principles calculation of elastic and thermodynamic properties of MgO and SrO under high pressure. *Physica B: Condensed Matter*, *373*(2), 334-340.
[82] Marx, D., &Hutter, J. (2000). Ab initio molecular dynamics: Theory and implementation. *Modern methods and algorithms of quantum chemistry*, *1*(301-449), 141.
[83] Kumar, M. (2002). Application of high pressure–high temperature equation of state for elastic properties of solids. *Physica B: Condensed Matter*, *311*(3-4), 340-347.
[84] Hohenberg, P., & Kohn, W. J. P. R. (1964). Density functional theory (DFT). *Phys. Rev*, *136*(1964), B864.
[85] Segall, M. D., Lindan, P. J., Probert, M. A., Pickard, C. J., Hasnip, P. J., Clark, S. J., & Payne, M. C. (2002). First-principles simulation: ideas, illustrations and the CASTEP code. *Journal of physics: condensed matter*, *14*(11), 2717.

[86] Perdew, J. P., &Zunger, A. (1981). Self-interaction correction to density-functional approximations for many-electron systems. *Physical Review B*, *23*(10), 5048.
[87] Perdew, J. P., Burke, K., &Ernzerhof, M. (1996). Generalized gradient approximation made simple. *Physical review letters*, *77*(18), 3865.
[88] Perdew, J. P., Ruzsinszky, A., Csonka, G. I., Vydrov, O. A., Scuseria, G. E., Constantin, L. A., ... & Burke, K. (2008). Restoring the density-gradient expansion for exchange in solids and surfaces. *Physical review letters*, *100*(13), 136406.
[89] Werner, W. (1984). Polynomial interpolation: Lagrange versus newton. *Mathematics of computation*, *43*(167), 205-217.
[90] Birch, F. (1978). Finite strain isotherm and velocities for single-crystal and polycrystalline NaCl at high pressures and 300 K. *Journal of Geophysical Research: Solid Earth*, *83*(B3), 1257-1268.
[91] Sahraoui, F. A., Arab, F., Zerroug, S., &Louail, L. (2008). First-principles study of structural and elastic properties of MgSe under hydrostatic pressure. *Computationalmaterials science*, *41*(4), 538-541.
[92] Mehl, M. J., Klein, B. M., &Papaconstantopoulos, D. A. (1995). Intermetallic compounds: principle and practice. *Principles*, *1*, 195-210.
[93] Schreiber, E., Anderson, O. L., Soga, N., & Bell, J. F. (1975). Elastic constants and theirmeasurement.
[94] Ravindran, P., Fast, L., Korzhavyi, P. A., Johansson, B., Wills, J., & Eriksson, O. (1998). Density functional theory for calculation of elastic properties of orthorhombic crystals: Application to TiSi 2. *Journal of Applied Physics*, *84*(9), 4891-4904.
[95] Christy, R. W. (1962). Solid State Physics, Vol. 12: Advances in Research and Applications. *American Journal of Physics*, *30*(12), 936-937.
[96] Kittel, C., & Holcomb, D. F. (1967). Introduction to solid state physics. *American Journal of Physics*, *35*(6), 547-548.
[97] Galperin, Y. M. (2002). Introduction to modern solid state physics. *PO Box*, *1048*, 181-206.
[98] Ahmad, J. F., &Mhmood, Z. R. (2020). Study the Effect of High Pressure and High Temperature on the Properties of Nacl-B1. *Journal of Education and Science*, *29*(2), 101-117.
[99]Sobolev, S. V., &Babeyko, A. Y. (1994). Modeling of mineralogical composition, density and elastic wave velocities in anhydrous magmatic rocks. *Surveys in geophysics*, *15*, 515-544.
[100] Karki, B. B., Stixrude, L., &Wentzcovitch, R. M. (2001).High-pressure elastic properties of major materials of Earth's mantle from first principles. *Reviews of Geophysics*, *39*(4), 507-534.
[101] Jeanloz, R., &Knittle, E. (1989).Density and composition of the lower mantle. *Philosophical Transactions of the Royal Society of London. Series A, Mathematical and Physical Sciences*, *328*(1599), 377-389.
[102] Voigt, W. J. T. L. (1928).A determination of the elastic constants for beta-quartz lehrbuch de kristallphysik. *Terubner Leipzig*, *40*, 2856-2860.
[103] Reuss, A. J. Z. A. M. M. (1929). Calculation of the flow limits of mixed crystals on the basis of the plasticity of monocrystals. *Z. Angew. Math. Mech*, *9*, 49-58.
[104] Hill, R. (1952).The elastic behaviour of a crystalline aggregate. *Proceedings of the Physical Society. Section A*, *65*(5), 349.